







## ORIGINAL ARTICLE

# Dual role of autotaxin as novel biomarker and therapeutic target in pancreatic neuroendocrine neoplasms

Tadashi Toyohara<sup>1</sup>  | Michihiro Yoshida<sup>1</sup>  | Katsuyuki Miyabe<sup>2</sup>  | Kazuki Hayashi<sup>1</sup> | Itaru Naitoh<sup>1</sup> | Hiromu Kondo<sup>1</sup> | Yasuki Hori<sup>1</sup> | Akihisa Kato<sup>1</sup>  | Kenta Kachi<sup>1</sup> | Go Asano<sup>1</sup> | Hidenori Sahashi<sup>1</sup> | Akihisa Adachi<sup>1</sup> | Kayoko Kuno<sup>1</sup> | Yusuke Kito<sup>1</sup> | Yoichi Matsuo<sup>3</sup>  | Hiromi Kataoka<sup>1</sup> 

<sup>1</sup>Department of Gastroenterology and Metabolism, Nagoya City University Graduate School of Medical Sciences, Nagoya, Japan

<sup>2</sup>Department of Gastroenterology, Japanese Red Cross Aichi Medical Center Nagoya Daini Hospital, Nagoya, Japan

<sup>3</sup>Department of Gastroenterological Surgery, Nagoya City University Graduate School of Medical Sciences, Nagoya, Japan

## Correspondence

Michihiro Yoshida, Department of Gastroenterology and Metabolism, Nagoya City University Graduate School of Medical Sciences, 1 Kawasumi, Mizuho-cho, Mizuho-ku, Nagoya 467-8601, Japan. Email: [mityoshi@med.nagoya-cu.ac.jp](mailto:mityoshi@med.nagoya-cu.ac.jp)

## Funding information

Japan Society for the Promotion of Science, Grant/Award Number: 21K20844 and 23K07444; Pancreas Research Foundation of Japan, Grant/Award Number: N/A

## Abstract

Pancreatic neuroendocrine neoplasms (panNENs) are rare pancreatic neoplasms, and descriptions of treatment remain limited. Autotaxin (ATX) is a secreted autocrine motility factor involved in the production of lysophosphatidic acid (LPA), a lipid mediator that promotes the progression of various cancers. The aim of this study was to clarify the importance of the ATX-LPA axis in panNENs and to confirm its contribution to panNEN progression using clinical data, cell lines, and a mouse model. Serum ATX level was higher in patients with panNEN than in patients with other pancreatic diseases (chronic pancreatitis, pancreatic ductal adenocarcinoma [PDAC], intraductal papillary mucinous neoplasm, autoimmune pancreatitis) and healthy controls, and 61% of clinical specimens stained strongly for ATX. In a case we encountered, serum ATX level fluctuated with disease progression. An in vitro study showed higher ATX mRNA expression in panNEN cell lines than in PDAC cell lines. Cell proliferation and migration in panNEN cell lines were stimulated via the ATX-LPA axis and suppressed by RNA interference or inhibitors. An in vivo study showed that intraperitoneal injection of GLPG1690, an ATX inhibitor, suppressed tumor progression in a xenograft model. These findings revealed that ATX expression is significantly elevated in panNEN and is related to the progression of panNEN. We showed the potential of ATX as a novel biomarker and therapeutic target.

## KEYWORDS

autotaxin, biomarker, lysophosphatidic acid, molecular target therapy, neuroendocrine tumor

**Abbreviations:** ATX, autotaxin; AUC, area under the curve; CCK-8, Cell Counting Kit-8; CI, confidence interval; CP, chronic pancreatitis; DMSO, dimethyl sulfoxide; FBS, fetal bovine serum; IHC, immunohistochemistry; IPMN, intraductal papillary mucinous neoplasm; LPA, lysophosphatidic acid; LPAR, lysophosphatidic acid receptor; LPC, lysophosphatidylcholine; MAPK, mitogen-activated protein kinase; NEC, neuroendocrine carcinoma; NEN, neuroendocrine neoplasm; NET, neuroendocrine tumor; NSE, neuron-specific enolase; panNEC, pancreatic neuroendocrine carcinoma; panNEN, pancreatic neuroendocrine neoplasm; PBS, phosphate-buffered saline; PCR, polymerase chain reaction; (PD, progressive disease; PDAC, pancreatic ductal adenocarcinoma; PR, partial response; ROC, receiver-operating characteristic; SD, stable disease; siNT, nontargeting siRNA; siRNA, small interfering RNA; WST-8, water-soluble tetrazolium salt.

This is an open access article under the terms of the [Creative Commons Attribution-NonCommercial](https://creativecommons.org/licenses/by-nc/4.0/) License, which permits use, distribution and reproduction in any medium, provided the original work is properly cited and is not used for commercial purposes.

© 2023 The Authors. *Cancer Science* published by John Wiley & Sons Australia, Ltd on behalf of Japanese Cancer Association.

## 1 | INTRODUCTION

Neuroendocrine neoplasms (NENs) are considered rare but have been increasing in recent years. According to statistical data from the United States, the annual age-adjusted incidence of neuroendocrine tumor (NET) was 6.98 per 100,000 individuals in 2012, representing an about sixfold increase from 1973.<sup>1</sup> Most NENs arise in the digestive system, in the small intestine, and rectum most frequently, followed by the pancreas.<sup>1</sup> Characteristically, nearly half of pancreatic NENs (panNENs) are found incidentally and frequently show regional invasion or distant metastasis.<sup>2</sup> Some blood-based biomarkers have been identified for panNENs, including insulin for insulinoma, gastrin for gastrinoma, and chromogranin A and neuron-specific enolase (NSE) for nonfunctional panNEN.<sup>3</sup> Although various investigations have been making efforts to discover more useful biomarkers, practically applicable results for use in clinical practice remain scarce.<sup>4-9</sup>

The treatment of patients with panNENs is wide ranging, with options including surgery, somatostatin analogs, molecularly targeted therapies, peptide receptor radionuclide therapy, and cytotoxic chemotherapy.<sup>10</sup> In recent years, multidisciplinary treatments have become more important. panNENs tend to develop relatively slowly, and sustained strategies with a number of regimens are important to control tumor development. In contrast, the number of molecularly targeted therapies against panNENs remain limited compared with other cancers. Novel targets for therapy are therefore needed.

Lysophosphatidic acid (LPA) is a lysophospholipid mediator with many physiological activities, including working as a growth factor for cancer cells.<sup>11</sup> Autotaxin (ATX) is a member of the ectonucleotide pyrophosphate and phosphatase family and is recognized as an autocrine motility-stimulating factor originally identified from melanoma cells.<sup>12</sup> ATX works as an enzyme in the hydrolysis of lysophosphatidylcholine (LPC) to LPA and has also been reported to contribute to cancer development via the ATX-LPA axis.<sup>13-18</sup> ATX has therefore attracted attention for potential use as a biomarker and therapeutic target.<sup>19-25</sup> Some studies have suggested the utility of ATX inhibitors for antitumor effects.<sup>26,27</sup> However, whether ATX and the ATX-LPA axis contribute to oncogenesis in panNENs remains unclear. The present study therefore investigated the role of the ATX-LPA axis in panNENs and clarified the oncogenic role of ATX with the aim of exploring its utility as a biomarker and therapeutic target for panNENs.

## 2 | MATERIALS AND METHODS

### 2.1 | Clinical samples

From May 2021 to May 2023, a total of 145 blood samples were collected from patients with pancreatic diseases at Nagoya City University Hospital. Underlying pathologies were pancreatic NET (panNET) in 14 patients (7 males, 7 females), pancreatic ductal adenocarcinoma (PDAC) in 62 (30 males, 32 females), chronic pancreatitis (CP) in 29 (26 males, 3 females), and intraductal papillary mucinous neoplasm

(IPMN) in 14 (5 males, 9 females), and there were 26 healthy controls (16 males, 10 females). Pathological specimens were obtained from patients with panNET treated between December 2010 and May 2021 at Nagoya City University Hospital ( $n=21$ ) and Japanese Red Cross Aichi Medical Center Nagoya Daini Hospital ( $n=15$ ). This retrospective study was approved by the institutional review board at Nagoya City University Hospital and Japanese Red Cross Aichi Medical Center Nagoya Daini Hospital (approval no. 60-22-0008) in accordance with the Declaration of Helsinki on ethical principles for medical research involving human participants. To measure serum ATX level, 0.5 mL of patients' serum was applied with a reagent of AIA-packCL (Tosoh Bioscience). According to the manufacturer's instruction, enzyme-linked immunosorbent assay was performed with AIA-CL2000 LA (Tosoh Bioscience).

### 2.2 | Cell cultures

The AsPC-1 and Capan-2 PDAC cell lines were purchased from RIKEN Cell Bank, QGP-1 pancreatic neuroendocrine carcinoma (panNEC) cell line was purchased from JCRB Cell Bank and the BON-1 panNET cell line was kindly provided by Dr. Keiichiro Sakuma (Division of Pathophysiology, Aichi Cancer Center Research Institute). QGP-1, AsPC-1, and Capan-2 cells were maintained in RPMI-1640 medium (FUJIFILM Wako Pure Chemical Corporation) and BON-1 cells in Dulbecco's Modified Eagle Medium DMEM (FUJIFILM Wako Pure Chemical Corporation). All media were supplemented with 10% fetal bovine serum (FBS) in an incubator with 5% CO<sub>2</sub> at 37°C.

### 2.3 | Cell viability assay

Cells were seeded at a density of  $5 \times 10^3$  cells per well on 96-well plates and cultured overnight. Next, cells were washed with phosphate-buffered saline (PBS) (Sigma Aldrich) and cultured in medium with 10% FBS condition. We added 15  $\mu\text{mol/L}$  of LPA for QGP-1, 1  $\mu\text{mol/L}$  of LPA for BON-1, 1  $\mu\text{mol/L}$  of LPC for QGP-1 and BON-1, and 10  $\mu\text{mol/L}$  of the ATX inhibitor GLPG1690 (MedChemExpress) for QGP-1 and BON-1 every 24 h. GLPG1690 was solubilized in dimethyl sulfoxide (DMSO) according to the protocol for GLPG1690 provided by the manufacturer. Cell viability was measured at fixed intervals using a Cell Counting Kit-8 (CCK-8) assay (Dojindo) and was evaluated by the absorption of water-soluble tetrazolium salt (WST-8). These experiments were independently conducted four times.

### 2.4 | Wound-healing assay (scratch assay)

A wound-healing assay was conducted to measure cell migration. A straight wound was scratched with a sterile 200- $\mu\text{L}$  pipette tip after the cells were cultured to confluence in 12-well plates. Next, 10  $\mu\text{mol/L}$  of GLPG1690 was added. In cases of RNA interference, the scratch was made 24 h after transfection of siATX. DMSO was

added for the control. The straight wound was photographed and measured under microscopy at 0 and 24 h. All experiments were independently conducted three times.

## 2.5 | In vivo experiments

Female nude mice (BALB/c Slc-nu/nu) were obtained from Japan SLC. All animal experiments were performed according to protocols approved by the Institutional Animal Care and Use Committee of Nagoya City University Graduate School of Medical Science. The xenograft model was made using mice at 5–6 weeks old by the implantation of  $5 \times 10^5$  BON-1 cells. Seven days after implantation, mice were allocated to two groups: control or GLPG1690 treatment. GLPG1690 was solubilized in a solvent. According to the protocol for GLPG1690, the solvent was made by adding each of the following solvents one by one: 5% DMSO (WAKO Pure Chemical Corporation); 40% polyethylene glycol 300; 5% Tween 80; and 50% saline. As previously described, 60 mg/kg of GLPG1690 was injected intraperitoneally every day, once a day.<sup>26,28,29</sup> Tumor volume was calculated as (depth) × (width) × (height) × 0.5. The body weight of mice and tumor size were measured twice a week. The mice were sacrificed on day 14. Tumor samples and serum were collected for further analyses. For the validation, we also carried out the same in vivo experiment using QGP-1 cells for analysis of the effect of GLPG1690;  $5 \times 10^5$  QGP-1 cells were implanted.

## 2.6 | Statistical analysis

All data were analyzed using Student's *t*-test and the Mann–Whitney *U*-test. Differences were considered statistically significant at the level of  $p < 0.05$ . Receiver-operating characteristic (ROC) analysis was used to calculate the area under the ROC curve (AUC) for serum ATX, and the AUC value with a 95% confidence interval (CI) was shown as representative value. All of the statistical analyses were undertaken using EZR software (version 1.61; Saitama Medical Center, Jichi Medical University). Data are expressed as the mean ± standard error.

We described fundamental materials and methods in Appendix S1.

## 3 | RESULTS

### 3.1 | High expression of ATX in panNEN

In this study using clinical specimens, we analyzed serum ATX levels and immunohistochemically stained pancreatic tissues for ATX. The serum level of ATX was significantly higher in panNEN (male,  $1.31 \pm 0.55$  mg/L; female,  $1.58 \pm 1.07$  mg/L) than in other pancreatic diseases in both males and females. Males: healthy controls,  $0.63 \pm 0.13$  mg/L ( $p < 0.01$ ); IPMN,  $0.62 \pm 0.27$  mg/L ( $p < 0.01$ ); PDAC,

$0.78 \pm 0.17$  mg/L ( $p < 0.01$ ); CP,  $0.64 \pm 0.09$  mg/L ( $p < 0.01$ ). Females: healthy controls,  $0.73 \pm 0.12$  mg/L ( $p < 0.01$ ); IPMN,  $0.77 \pm 0.12$  mg/L ( $p < 0.05$ ); PDAC,  $0.90 \pm 0.25$  mg/L ( $p < 0.05$ ); and CP,  $0.57 \pm 0.03$  mg/L ( $p < 0.05$ ) (Figure 1A). ROC curve analysis was performed to calculate the AUC for the biomarker to diagnose panNEN. These data showed significant differences between panNEN and PDAC/healthy controls: panNEN and PDAC/healthy control in male, AUC = 0.855 (95% CI, 0.670–1.000)/0.951 (0.869–1.000); panNEN and PDAC/healthy control in female, 0.795 (0.594–0.995)/0.921 (0.794–1.000) (Figure S1). Immunohistochemical analyses showed that ATX was strongly expressed in tumor cells on the membrane and in plasma, although normal pancreatic duct epithelial cells did not express ATX (Figure 1B). In 61% of cases, ATX was highly expressed. We further compared characteristics between high- and low-expression groups. For all the terms we considered, no significant differences were seen between the two groups (Table 1), indicating that the production of ATX by tumor cells might not be independent of tumor status and characteristics.

We also monitored serum ATX levels in a case (Figure 2). This 70-year-old woman had panNET G2 and multiple metastases in the liver (Figure 2A). Serum ATX level was 2.98 mg/L at diagnosis, and streptozocin was administered as the first-line therapy. ATX level gradually increased along with exacerbation of findings on imaging (Figure 2B), reaching 4.14 mg/L 6 months after starting treatment. Everolimus was then administered as the second-line therapy. This achieved rapid cytoreduction (Figure 2C), and the tumor response was judged as partial response 2 months after switching drugs. ATX level decreased to 1.22 mg/L along with the tumor response assessed on imaging. This second-line therapy was effective for a limited time; then, the tumor gradually started to progress again. The serum ATX level rose to 2.51 mg/L by 6 months after starting everolimus. Unfortunately, the patient experienced rapid, uncontrollable tumor progression 15 months after diagnosis. The serum ATX level showed a transition paralleling both tumor progression and serum level of NSE (Figure 2D).

In vitro, relative mRNA expression levels of ATX were much higher in cell lines of panNEN (QGP-1,  $1.00 \pm 0.67$ ; BON-1,  $2961 \pm 763$ ) than in PDAC cell lines (AsPC-1,  $0.65 \pm 1.57$ ; Capan-2,  $0.07 \pm 0.37$ ) (Figure 1C), showing that panNEN itself expressed abundant ATX. These results indicate that panNEN cells are highly expressive of ATX, and transitions in serum levels of ATX reflect the tumor burden on imaging.

### 3.2 | Lysophosphatidic acid contributes to proliferation via LPA receptor by phosphorylating ERK1/2 in panNEN

Autotaxin produces LPA from LPC and induces various effects via binding with LPA receptor (LPAR). Cell proliferation was significantly promoted by LPA administration in QGP-1 (relative cell number at 48 h:  $2.089 \pm 0.10$  vs.  $2.33 \pm 0.06$ ,  $p < 0.01$ ) and BON-1 (48 h:  $2.76 \pm 0.02$  vs.  $3.28 \pm 0.10$ ,  $p < 0.01$ ) (Figure 3A). The

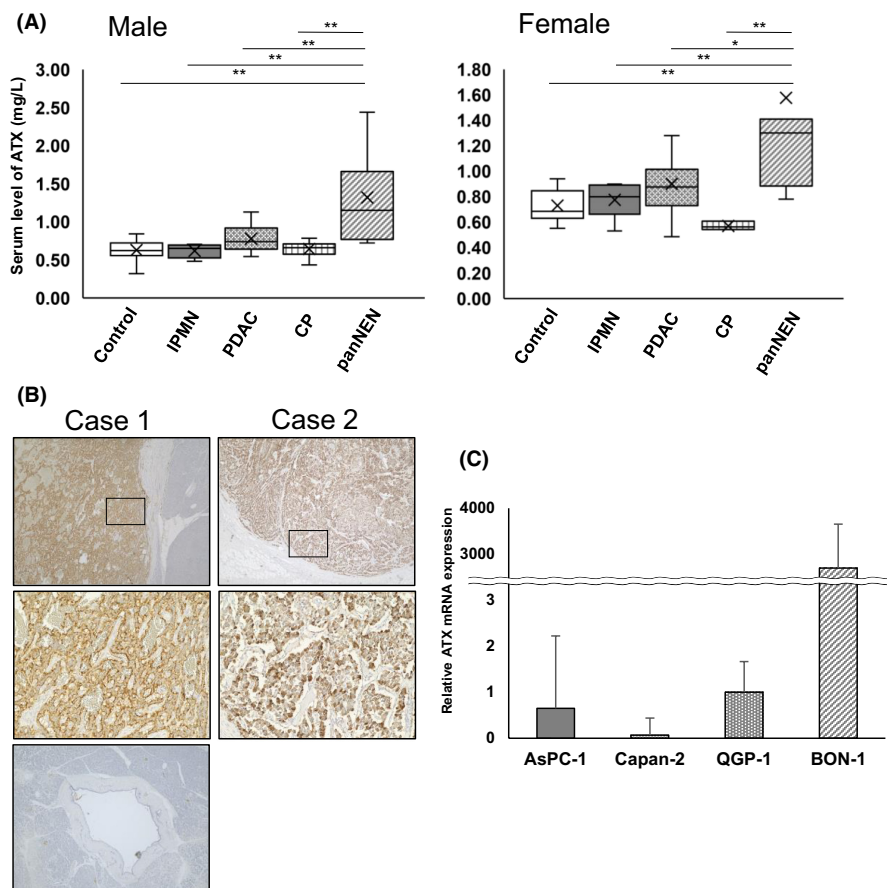


**FIGURE 1** Pancreatic neuroendocrine neoplasm (panNEN) shows high expression of autotaxin (ATX). (A) Serum ATX level in panNEN, intraductal papillary mucinous neoplasm (IPMN), pancreatic ductal adenocarcinoma (PDAC), chronic pancreatitis (CP) and healthy control by sex. The number of patients with each pathology was: in males, panNEN in 7, IPMN in 5, PDAC in 30, CP in 26, with 16 healthy controls; in females, panNEN in 7, IPMN in 9, PDAC in 32, CP in 3, with 10 healthy controls. Bars, standard error; \* $p < 0.05$ , \*\* $p < 0.01$ . (B) Representative images of immunohistochemical staining for ATX expression in panNEN. Insets show magnified views of boxed areas. Magnification:  $\times 40$ ; inset  $\times 200$ . Case 1 was a patient with panNET G2, and case 2 involved neuroendocrine carcinoma. Bottom: normal pancreatic duct from the same slide in case 1. (C) Relative mRNA expression of ATX in AsPC-1 ( $n = 3$ ), Capan-2 ( $n = 4$ ), QGP-1 ( $n = 4$ ), and BON-1 ( $n = 3$ ). Bars, standard error.

mitogen-activated protein kinase (MAPK) pathway has been reported as a major downstream pathway of LPA-LPAR signaling.<sup>30</sup> In our study, phosphorylation of ERK1/2 was increased by LPA activation in QGP-1 and BON-1 (Figure 3B). These results indicate that LPA promotes cell proliferation via MAPK signaling in panNEN cells. LPC is the precursor to LPA that is hydrolyzed by ATX. We confirmed a significant upregulation of cell proliferation by LPC administration in QGP-1 (48 h:  $2.21 \pm 0.10$  vs.  $2.74 \pm 0.02$ ,  $p < 0.01$ ) and BON-1 (48 h:  $4.53 \pm 0.09$  vs.  $5.15 \pm 0.15$ ,  $p < 0.01$ ) (Figure 3C). LPC also induced ERK1/2 phosphorylation as well as LPA (Figure 3D). LPC-induced phosphorylation in these two cell lines was greater than that in Capan-2 which showed weaker AXT mRNA expression (Figure S2). These results confirmed that the LPA precursor, LPC, achieved the same biological activation as LPA.

Next, we evaluated the function of LPAR using small interfering RNA (siRNA) transfection. We analyzed mRNA expressions of LPA receptors 1 (LPAR1), 2 (LPAR2), and 3 (LPAR3) in four cell lines. Figure 3E shows relative expression levels of each receptor. LPAR2 was predominantly expressed in QGP-1 and BON-1 as compared with the AsPC-1 cell line, but significant expressions of LPAR1 and LPAR3 were also confirmed. We investigated whether repression of each LPAR affected cell proliferation. Knockdown efficiency of each LPA receptor was confirmed to be around 20% (Figure 3G). Each of siLPAR1, siLPAR2, and siLPAR3 significantly suppressed cell proliferation in QGP-1 (48 h: siLPAR1,  $3.05 \pm 0.15$

vs.  $1.65 \pm 0.07$ ,  $p < 0.01$ ; siLPAR2,  $7.58 \pm 0.35$  vs.  $4.94 \pm 0.38$ ,  $p < 0.01$ ; siLPAR3,  $3.07 \pm 0.04$  vs.  $1.91 \pm 0.03$ ,  $p < 0.01$ ) and BON-1 (48 h: siLPAR1,  $5.93 \pm 0.05$  vs.  $4.87 \pm 0.35$ ,  $p < 0.01$ ; siLPAR2,  $5.47 \pm 0.17$  vs.  $2.51 \pm 0.10$ ,  $p < 0.01$ ; siLPAR3,  $4.03 \pm 0.19$  vs.  $3.40 \pm 0.03$ ,  $p < 0.01$ ) (Figure 3H–M). These results provide important insights into the significance of LPA-LPAR signaling in the progression of panNEN.

### 3.3 | Inhibition of ATX suppresses cell proliferation and migration in panNEN

We conducted cell viability and wound-healing assays to assess the effects of ATX on cell proliferation and migration in panNEN. Two approaches were applied to achieve ATX inhibition. First, we inhibited ATX expression using RNA interference. Knockdown efficiency of ATX in both QGP-1 and BON-1 was confirmed to be under 20% (Figure 4A,B). Cell proliferation of siATX was significantly suppressed compared with control in QGP-1 (48 h,  $10.8 \pm 0.49$  vs.  $7.93 \pm 0.18$ ,  $p < 0.01$ ) and BON-1 (48 h,  $3.89 \pm 0.01$  vs.  $3.02 \pm 0.07$ ,  $p < 0.01$ ) (Figure 4C). In a scratch assay of BON-1 cells, silencing ATX significantly suppressed the migration rate compared with control (migration rate:  $0.32 \pm 0.05$  vs.  $0.11 \pm 0.01$ ,  $p < 0.01$ ). (Figure 4D,E).

Second, we administered GLPG1690 as an inhibitor of ATX. GLPG1690 treatment achieved significant suppression of proliferation

TABLE 1 Clinicopathological features.

Variables	Number	ATX expression		p-Values
		Low (n = 14)	High (n = 22)	
Sex				
Male	18	8	10	0.733
Female	18	6	12	
Age, year				
≥60	18	7	11	1
<60	18	7	11	
Tumor location				
Head	11	6	5	0.273
Body/tail	25	8	17	
Tumor size, cm				
≥2	15	7	8	0.701
<2	20	7	13	
TNM stage				
I–II	21	8	13	1
III–IV	15	6	9	
Ki-67 index, %				
≥20	4	3	1	0.277
<20	32	11	21	
Type				
Functional	8	2	6	0.441
Nonfunctional	28	12	16	
Grading				
NET G1	21	8	13	0.741
NET G2	10	3	7	
NET G3	2	1	1	
NEC	3	2	1	

Abbreviations: ATX, autotaxin; NEC, neuroendocrine carcinoma; NET, neuroendocrine tumor.

compared with control in QGP-1 (relative cell number at 48h:  $2.81 \pm 0.10$  vs.  $1.89 \pm 0.13$ ,  $p < 0.01$ ) and BON-1 (48h:  $4.14 \pm 0.09$  vs.  $1.17 \pm 0.02$ ,  $p < 0.01$ ) (Figure 4F). In migration assays, migration in the GLPG1690 group was significantly suppressed compared with control (Figure 4G), and the migration rate was also reduced with GLPG1690 ( $0.29 \pm 0.02$  vs.  $0.20 \pm 0.0$ ,  $p < 0.05$ ) (Figure 4H). GLPG1690 treatment in addition to LPC administration attenuated phosphorylation of ERK1/2 (Figure 4I).

These results suggest that inhibition of ATX decreased LPA-derived signal transduction and suppressed cell proliferation and migration.

### 3.4 | Autotaxin inhibitor suppresses panNEN progression in a murine xenograft model

In our vivo study, we subcutaneously implanted BON-1 cells into nude mice and intraperitoneally injected 60mg/kg of GLPG1690 dissolved in DMSO once a day for 13 days. Tumor size of BON-1 was significantly smaller with GLPG1690 treatment compared

with control, which were injected equivalent amount of DMSO in terms of both volume (day 13:  $197.5 \pm 28.7$  vs.  $110.4 \pm 18.0 \text{ mm}^3$ ,  $p < 0.01$ ) and weight (day 13:  $0.21 \pm 0.03$  vs.  $0.10 \pm 0.02 \text{ g}$ ,  $p < 0.01$ ) (Figure 5A,B). In the result of the experiment using QGP-1 for validation, the tumor volume of QGP-1 with GLPG1690 treatment was significantly smaller than that of control (day 13:  $324.7 \pm 28.9$  vs.  $185.8 \pm 39.9 \text{ mm}^3$ ,  $p < 0.05$ ). The tumor weight tended to be lighter (day 13:  $0.34 \pm 0.04$  vs.  $0.20 \pm 0.05 \text{ g}$ ,  $p = 0.065$ ) (Figure S3).

Immunohistochemistry (IHC) analysis was performed using tumor samples (Figure 5C). Rates of Ki-67-positive cells and phosphorylated ERK1/2-positive cells were significantly lower in the GLPG1690 group than in the control group (Ki-67:  $50.4\% \pm 2.1\%$  vs.  $38.2\% \pm 1.6\%$ ,  $p < 0.01$ ; pERK1/2:  $37.4\% \pm 2.9\%$  vs.  $25.5\% \pm 4.1\%$ ,  $p < 0.05$ ) (Figure 5D). In contrast, the rate of cleaved caspase-3-positive cells showed no significant difference between groups (data not shown). These results showed that ATX inhibitor suppressed tumor proliferation by inhibiting LPA production and subsequent MAPK signaling, in line with the results of the previous vitro study.

## 4 | DISCUSSION

Lysophosphatidic acid is a lysophospholipid mediator that shows various physiological activities. Particularly in cancer cells, LPA stimulates tumor cell proliferation, migration, and invasion via LPA receptors and is associated with cancer survival.<sup>25</sup> The ATX-LPA axis has been considered an important pathway and many researchers have investigated the possibility for targeted therapies against various cancers.

The present study first investigated serum ATX levels in a number of pancreatic diseases to reveal that serum ATX levels were significantly increased in patients with panNEN than in patients with other diseases. ATX has been reported to be highly expressed and has recently gained popularity as a biomarker in many kinds of cancer, such as lung cancer,<sup>31</sup> breast cancer,<sup>20</sup> thyroid cancer,<sup>32</sup> endometrial cancer,<sup>21</sup> and pancreatic cancer.<sup>14,19,33,34</sup> In our study, serum ATX levels in pancreatic cancer patients were significantly higher than in healthy controls, in line with previous studies. Furthermore,

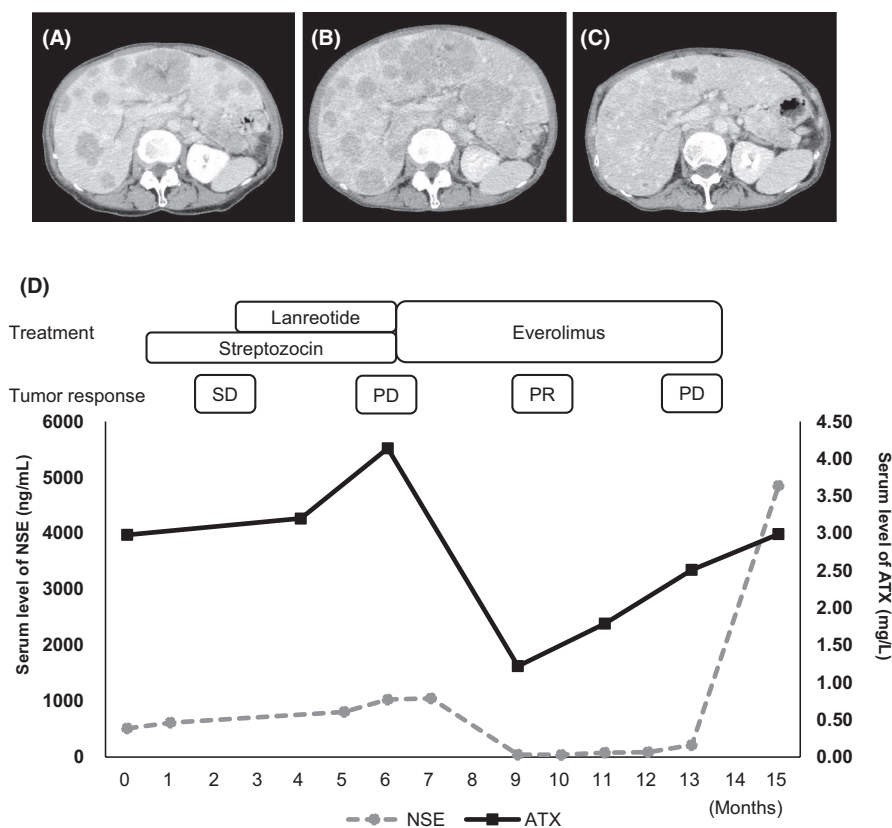


**FIGURE 2** Autotaxin (ATX) works as a biomarker of both tumor presence and tumor response. (A, B, C) Serial enhanced CT imaging showing tumor progress (A) at diagnosis, (B) with PD at 6 months after diagnosis, and (C) with PR at 9 months after diagnosis. (D) Clinical course of the patient from diagnosis (0 months). The left-side scale shows serum levels of neuron-specific enolase (NSE). The right-side scale shows serum levels of ATX. Above the graph, drugs for treatment and tumor response are shown. SD, stable disease; PD, progressive disease; PR, partial response.

**FIGURE 3** Lysophosphatidic acid (LPA) and lysophosphatidylcholine (LPC) promote cell proliferation and signal transduction in pancreatic neuroendocrine neoplasm (panNEN) cell lines (A). PanNEN cells (QGP-1 and BON-1) were cultured in media without FBS with 15  $\mu$ mol/L LPA in QGP-1 and 1  $\mu$ mol/L LPA in BON-1 (LPA [+]) or equivalent amount of 0.1% BSA (LPA [-]). Number of cells was measured daily by CCK-8. Representative results from four independent experiments are shown. Data represent mean of LPA (+) and LPA (-). Bars, standard error; \* $p < 0.05$ , \*\* $p < 0.01$ . (B) PanNEN cells were treated with LPA (10  $\mu$ mol/L) for the indicated duration. Western blotting showed analysis of ERK1/2 phosphorylation in QGP-1 and BON-1 cells. Quantification of p-ERK1/2 expression normalized to total ERK levels using ImageJ software. (C) panNEN cells (QGP-1 and BON-1) were cultured in media without FBS with 1  $\mu$ mol/L LPC in QGP-1 and BON-1 (LPC [+]) or an equivalent amount of 0.1% BSA (LPC [-]). Cell numbers were measured daily using CCK-8. Representative results from four independent experiments are shown. Data represent mean values for LPC (+) and LPC (-). Bars, standard error; \* $p < 0.05$ , \*\* $p < 0.01$ . (D) panNEN cells were treated with 10  $\mu$ mol/L LPC for the indicated duration. Western blotting showed the analysis of ERK1/2 phosphorylation in QGP-1 and BON-1 cells. (E) Relative mRNA expression of LPA receptor subtypes in AsPC-1, Capan-2, QGP-1, and BON-1. Data gained from three independent experiments represent mean relative mRNA expressions of each LPA receptor subtype in AsPC-1, Capan-2, QGP-1, and BON-1 cell lines. Bars, standard error. (F, G) Knockdown efficiency of siLPAR in QGP-1 (F) and BON-1 (G). Knockdown efficiency of siLPAR was as follows: QGP-1: LPAR1 (14.4%), LPAR2 (24.7%), and LPAR3 (32.7%); BON-1: LPAR1 (26.5%), LPAR2 (18.2%), and LPAR3 (11.4%). Data gained from three independent experiments represent mean relative mRNA expressions of each LPA receptor subtype in QGP-1 and BON-1. Bars, standard error; \* $p < 0.05$ , \*\* $p < 0.01$ . (H-M) PanNEN cells with transduction of RNA interference for LPA receptor subtypes cultured in complete media with 10% FBS. Number of cells was counted daily using CCK-8. Data gained from eight independent experiments represent means for control group as nontargeted small interfering RNA (siRNA) and the treatment group with siRNAs siLPAR1 (H, I), siLPAR2 (J, K), and siLPAR3 (L, M). Bars, standard error; \* $p < 0.05$ , \*\* $p < 0.01$ .

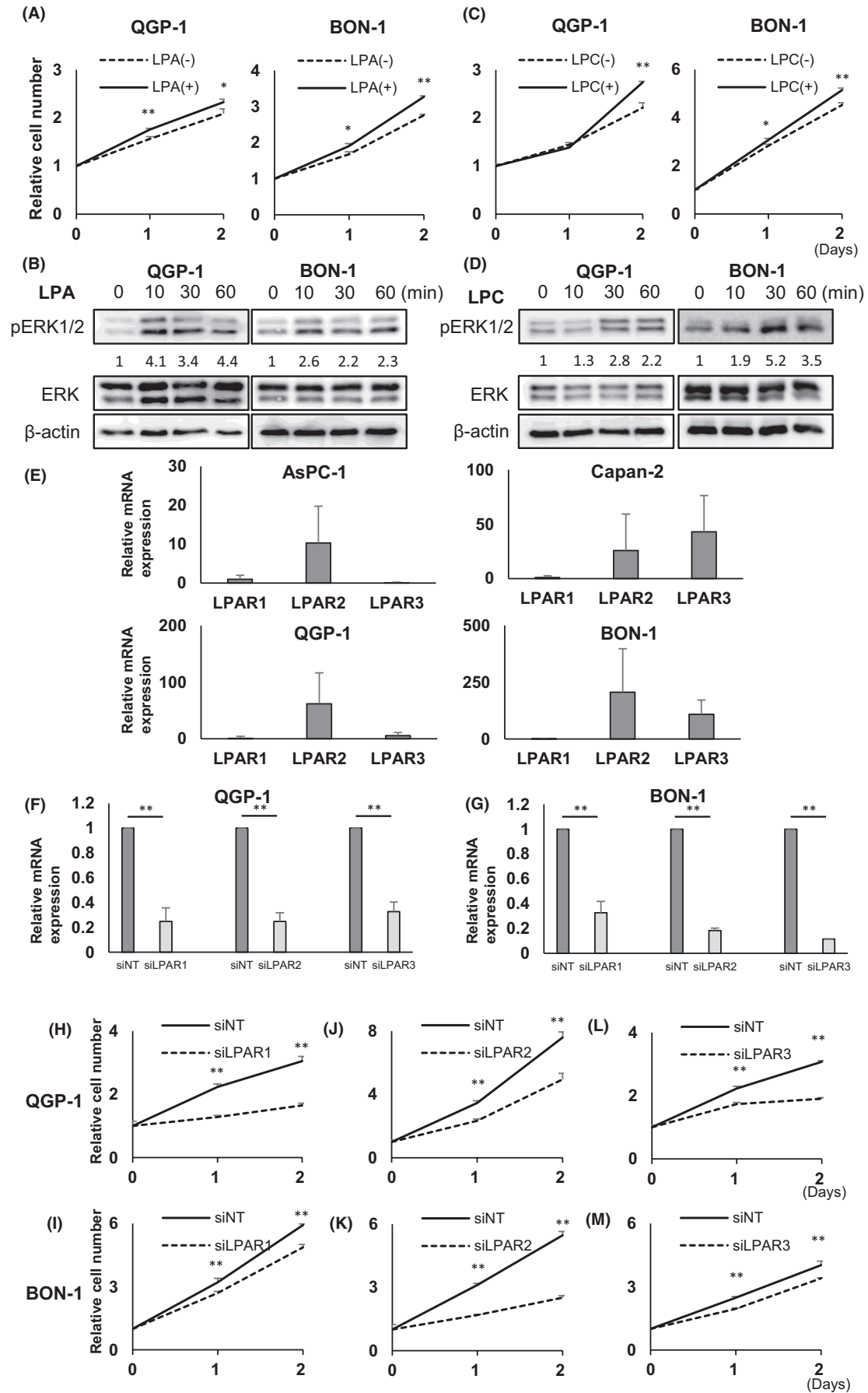






**FIGURE 4** Autotaxin (ATX) inhibition suppresses proliferation and migration in QGP-1 and BON-1. (A, B) Knockdown efficiency of siLPA in QGP-1 (A) and BON-1 (B). Knockdown efficiency of siATX was: QGP-1, 30.0%; BON-1, 11.6%. Data gained from three independent experiments represent means for relative mRNA expression of ATX in QGP-1 and BON-1. Bars, standard error; \* $p < 0.05$ , \*\* $p < 0.01$ . (C) Cell proliferation by RNA interference of ATX in QGP-1 and BON-1. Data represent means for control group with nontargeting siRNA (siNT) ( $n = 4$ ) and the treatment group with siATX ( $n = 4$ ). Bars, standard error; \* $p < 0.05$ , \*\* $p < 0.01$ . (D) Representative images obtained at 0 and 24 h after scratch wound made in confluent monolayers of BON-1 cells. At 24 h before scratch, BON-1 cells were transfected with siNT or siRNA for ATX (siATX). (E) Quantification of wound-healing assay in BON-1 cells. Data represent means of three independent experiments. Bars, standard error; \* $p < 0.05$ , \*\* $p < 0.01$ . (F) Cell proliferation by ATX inhibitor (GLPG1690) in QGP-1 and BON-1. Data represent means of the control group with dimethyl sulfoxide (DMSO) ( $n = 4$ ) and treatment group with GLPG1690 ( $n = 4$ ). Daily treatment was GLPG1690 at 10  $\mu\text{mol/L}$  in QGP-1 and BON-1 or equivalent amount of DMSO. Bars, standard error; \* $p < 0.05$ , \*\* $p < 0.01$ . (G) Representative images obtained at 0 and 24 h after scratch wound was made in confluent monolayers of BON-1 cells. Just after scratching, BON-1 cells were treated with 10  $\mu\text{mol/L}$  of DMSO or GLPG1690. (H) Quantification of wound-healing assay in BON-1 cells. Data represent means of four independent experiments. Bars, standard error; \* $p < 0.05$ , \*\* $p < 0.01$ . (I) Western blotting analysis of ERK phosphorylation after addition of GLPG1690 and 10  $\mu\text{mol/L}$  of lysophosphatidylcholine. Concentrations of GL PG1690 were 0, 10, 20, and 40  $\mu\text{mol/L}$ , respectively.

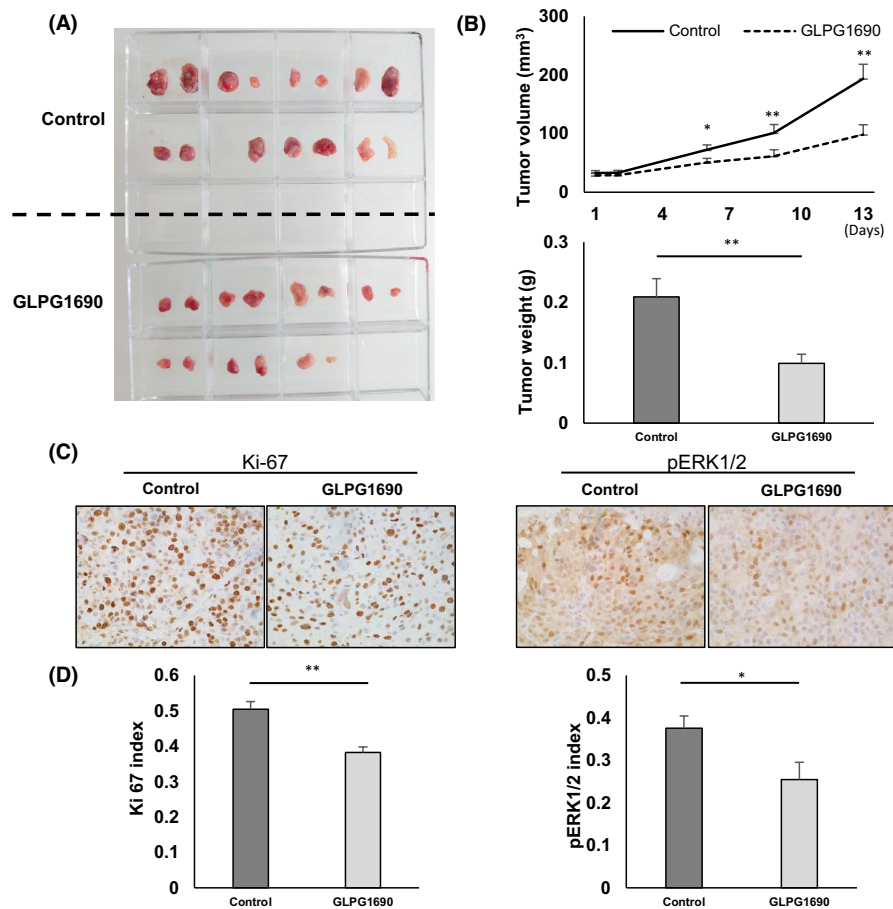


**FIGURE 5** Blocking autotaxin (ATX) attenuates tumor growth. Assessment of an in vivo experiment using a xenograft model. (A) Representative images of whole tumor exenterated from nude mice with BON-1 implantation and addition of dimethyl sulfoxide (DMSO) or GLPG1690 on day 14 after beginning drug treatment. The solvent was made by adding each solvent one by one: 5% DMSO (WAKO Pure Chemical Corporation), 40% polyethylene glycol 300, and 5% Tween 80 and 50% saline. GLPG1690 solubilized in the solvent above was injected intraperitoneally at the dose of 60 mg/kg body weight once a day. (B) Quantification of tumor volume and weight. Data represent mean values from the control group ( $n = 15$ ) and GLPG1690 group ( $n = 14$ ). Bars, standard error; \* $p < 0.05$ , \*\* $p < 0.01$ . (C) Representative immunohistochemical images of Ki-67 and p-ERK1/2 in the control and GLPG1690 groups. (D) Quantification of Ki-67 and p-ERK1/2 index in the control and GLPG1690 groups. Data representative means of the control group and GLPG1690 group. Bars, standard error; \* $p < 0.05$ , \*\* $p < 0.01$ .

serum ATX levels were significantly higher in panNEN patients than in those with pancreatic cancer. We successfully revealed panNEN as a key disease in which serum ATX level could work as a diagnostic biomarker, among a number of pancreatic diseases.

Some studies have suggested a relationship between ATX and oncogenesis. Previous studies have shown that ATX expression as evaluated by IHC is upregulated in various types of cancers and high ATX expression correlates with cancer prognosis. Immunohistochemical

analyses in our study showed high expression of ATX by tumor cells in 61% of panNEN cases. Unexpectedly, ATX expression in tumor tissue did not correlate with the degree of clinical malignancy in our immunohistochemical analysis, but ATX could be widely expressed in a certain number of panNEN tumors regardless of stage or grade. This seems to differ from previous reports but might depend on the type of solid tumor. In fact, Singh et al. reported that ATX expression was decreased in a poor-prognosis group of patients with melanoma, representing contradictory evidence.<sup>35</sup> We also revealed significant mRNA expression of ATX in two panNEN cell lines, supporting the notion that significant amounts of ATX are generated from panNEN tumor cells. Based on the accumulating evidence, we expected that in some panNEN patients, increases in serum ATX level could depend on the amount of tumor cells that could produce ATX. We encountered a case in which serum ATX levels showed an interesting trend. These results suggest that serum ATX level offers a useful biomarker for not only diagnosis but also follow-up of panNEN. To the best of our knowledge, this is the first report to investigate serum ATX level as a biomarker for panNEN. These novel discoveries in clinical research strongly motivated us to investigate the role of ATX in panNENs using laboratory-based research.

Autotaxin catalyzes the hydrolysis of LPA from LPC, which shows various physiological activities by stimulating the LPAR. The relationship between the ATX-LPA axis and cancer progression has been observed in various cancers, but few reports have examined NETs. In our study, LPA and LPC stimulation both activated cell proliferation and phosphorylation of ERK1/2 in two panNEN cell lines. This reveals that ligand-derived LPAR activation promotes proliferation via the MAPK signaling pathway, in line with previous studies.<sup>21,24,25,36,37</sup> In the present study, the dominant LPA receptors, LPAR1–3, were confirmed to be expressed at sufficient amounts in panNEN cell lines as well as pancreatic cancer cell lines, and knockdown of LPAR1–3 suppressed proliferation, implying that each of LPAR1–3 in panNEN cells can be categorized as oncogenic factors and that comprehensive regulation targeting all LPARs could be expected to provide more effective treatment for panNEN. Treatments targeting LPA are theoretically worthy of note. However, controlling LPA itself is difficult because LPA is an unstable mediator with a short half-life of approximately 3 min.<sup>38</sup> From this perspective, ATX could enter the limelight as an enzyme with an important role in stably generating a significant amount of LPA.

Many ATX inhibitors are known,<sup>34,39,40</sup> but few have been applied to clinical trials. Among them, GLPG1690 has been applied to clinical-phase trials in idiopathic pulmonary fibrosis and could be expected to show promise in future clinical studies of panNEN.<sup>29,41</sup>

The present study had various limitations, particularly the small clinical sample size. The number of NEC was too small to analyze and reach any conclusion with statistical significance. Only three cases of NEC were enrolled for immunohistochemical analysis and none for serum ATX analysis in the present study. Many reports have discussed the differences between NET and NEC and have suggested differences from a variety of perspectives.<sup>42–44</sup> In

the present study, the rate of ATX positivity in IHC analysis was 64% for NET and 33% for NEC. The positive rate for ATX seems higher in NET than in NEC, although no significant difference was seen between two groups, which might be affected by the small sample size. Moreover, *in vitro* experiments showed that relative ATX expression by transcription polymerase chain reaction (PCR) analysis was much higher in BON-1 ( $2962 \pm 763$ ) than in QGP-1 ( $1.00 \pm 0.67$ ). These data indicated that NET tumors might show greater ATX expression than NEC tumors. Nevertheless, an *in vitro* and *in vivo* study showed that targeting ATX could hold potential as a molecularly targeted therapy in the QGP-1 NEC cell line and BON-1 NET cell line. We also encountered a valuable case of NEC in which immunohistochemical analysis showed high ATX expression in the tumor. These results imply that ATX could play a common role in the oncogenesis of both NET and NEC. The detailed characteristics of ATX in NEC remain to be clarified. These limitations could be overcome by future analyses with a larger sample size. Clinical benefits beyond differential diagnosis, such as treatment selection and prediction of treatment efficacy, would be also expected to be clarified in future research.

In conclusion, we showed that ATX expression is significantly high in panNEN and could contribute to its progression. We also showed the potential of ATX as a novel biomarker and therapeutic target for panNEN.

## AUTHOR CONTRIBUTIONS

**Tadashi Toyohara:** Conceptualization; data curation; formal analysis; investigation; methodology; project administration; resources; visualization; writing – original draft. **Michihiro Yoshida:** Conceptualization; funding acquisition; investigation; project administration; resources; supervision; writing – review and editing. **Katsuyuki Miyabe:** Data curation; resources. **Kazuki Hayashi:** Data curation; resources; supervision. **Itaru Naitoh:** Data curation; project administration; resources. **Hiromu Kondo:** Data curation; funding acquisition. **Yasuki Hori:** Data curation; investigation. **Akihisa Kato:** Data curation; investigation; validation. **Kenta Kachi:** Data curation; investigation. **Go Asano:** Data curation; investigation. **Hidenori Sahashi:** Investigation; validation. **Akihisa Adachi:** Data curation; investigation. **Kayoko Kuno:** Data curation; investigation. **Yusuke Kito:** Data curation; investigation. **Yoichi Matsuo:** Resources; supervision. **Hiromi Kataoka:** Project administration; supervision; writing – review and editing.

## ACKNOWLEDGMENTS

We wish to thank Dr. Keiichiro Sakuma for providing the BON-1 cell line. This study was supported by grants from the Japan Society for the Promotion of Science (KAKENHI grant no. 21K20844 and 23K07444) and Pancreas Research Foundation of Japan.

## FUNDING INFORMATION

Japan Society for the Promotion of Science (KAKENHI grant no. 21K20844 and 23K07444) and Pancreas Research Foundation of Japan.

## CONFLICT OF INTEREST STATEMENT

The authors declare no conflict of interest.

## ETHICS STATEMENTS

Approval of the research protocol by an Institutional Reviewer Board: This study was approved by the institutional review board at Nagoya City University Hospital and Japanese Red Cross Aichi Medical Center Nagoya Daini Hospital (approval no. 60-22-0008) in accordance with the Declaration of Helsinki on ethical principles for medical research involving human participants.

Informed Consent: N/A.

Registry and the Registration: N/A.

Animal Studies: All animal experiments were performed according to protocols approved by the Institutional Animal Care and Use Committee of Nagoya City University Graduate School of Medical Science.

## ORCID

Tadashi Toyohara  <https://orcid.org/0009-0002-2302-0883>

Michihiro Yoshida  <https://orcid.org/0000-0002-4167-2781>

Katsuyuki Miyabe  <https://orcid.org/0000-0002-4915-9835>

Akihisa Kato  <https://orcid.org/0000-0002-7733-7854>

Yoichi Matsuo  <https://orcid.org/0000-0001-9654-6080>

Hiroimi Kataoka  <https://orcid.org/0000-0001-9491-0723>

## REFERENCES

- Dasari A, Shen C, Halperin D, et al. Trends in the incidence, prevalence, and survival outcomes in patients with neuroendocrine tumors in the United States. *JAMA Oncol.* 2017;3:1335-1342.
- Masui T, Ito T, Komoto I, Uemoto S. Recent epidemiology of patients with gastro-entero-pancreatic neuroendocrine neoplasms (GEP-NEN) in Japan: a population-based study. *BMC Cancer.* 2020;20:1104.
- Modlin IM, Oberg K, Taylor A, Drozdov I, Bodei L, Kidd M. Neuroendocrine tumor biomarkers: current status and perspectives. *Neuroendocrinology.* 2014;100:265-277.
- Kidd M, Drozdov I, Modlin I. Blood and tissue neuroendocrine tumor gene cluster analysis correlate, define hallmarks and predict disease status. *Endocr Relat Cancer.* 2015;22:561-575.
- Liu E, Paulson S, Gulati A, et al. Assessment of NETest clinical utility in a U.S. registry-based study. *Oncologist.* 2019;24:783-790.
- Malczewska A, Oberg K, Kos-Kudla B. NETest is superior to chromogranin a in neuroendocrine neoplasia: a prospective ENETS CoE analysis. *Endocr Connect.* 2021;10:110-123.
- Modlin IM, Drozdov I, Alaimo D, et al. A multianalyte PCR blood test outperforms single analyte ELISAs (chromogranin a, pancreastatin, neurokinin a) for neuroendocrine tumor detection. *Endocr Relat Cancer.* 2014;21:615-628.
- Pavel M, Jann H, Prasad V, Drozdov I, Modlin IM, Kidd M. NET blood transcript analysis defines the crossing of the clinical Rubicon: when stable disease becomes progressive. *Neuroendocrinology.* 2017;104:170-182.
- Modlin IM, Kidd M, Malczewska A, et al. The NETest: the clinical utility of multigene blood analysis in the diagnosis and management of neuroendocrine tumors. *Endocrinol Metab Clin North Am.* 2018;47:485-504.
- Scott AT, Howe JR. Evaluation and management of neuroendocrine tumors of the pancreas. *Surg Clin North Am.* 2019;99:793-814.
- Kano K, Aoki J, Hla T. Lysophospholipid mediators in health and disease. *Annu Rev Pathol.* 2022;17:459-483.
- Stracke ML, Krutzsch HC, Unsworth EJ, et al. Identification, purification, and partial sequence analysis of autotaxin, a novel motility-stimulating protein. *J Biol Chem.* 1992;267:2524-2529.
- Benesch MGK, Tang X, Brindley DN. Autotaxin and breast cancer: towards overcoming treatment barriers and sequelae. *Cancers (Basel).* 2020;12:374.
- Auciello FR, Bulusu V, Oon C, et al. A stromal lysolipid-autotaxin signaling axis promotes pancreatic tumor progression. *Cancer Discov.* 2019;9:617-627.
- Federico L, Jeong KJ, Vellano CP, Mills GB. Thematic review series: phospholipases: central role in lipid signaling and disease autotaxin, a lysophospholipase D with pleomorphic effects in oncogenesis and cancer progression. *J Lipid Res.* 2016;57:25-35.
- Hauck T, Kadam S, Heinz K, et al. Influence of the autotaxin-lysophosphatidic acid axis on cellular function and cytokine expression in different breast cancer cell lines. *Sci Rep.* 2022;12:5565.
- Lee D, Suh DS, Lee SC, Tigyi GJ, Kim JH. Role of autotaxin in cancer stem cells. *Cancer Metastasis Rev.* 2018;37:509-518.
- Tigyi GJ, Yue J, Norman DD, et al. Regulation of tumor cell - microenvironment interaction by the autotaxin-lysophosphatidic acid receptor axis. *Adv Biol Regul.* 2019;71:183-193.
- Nakai Y, Ikeda H, Nakamura K, et al. Specific increase in serum autotaxin activity in patients with pancreatic cancer. *Clin Biochem.* 2011;44:576-581.
- Shao Y, Yu Y, He Y, Chen Q, Liu H. Serum ATX as a novel biomarker for breast cancer. *Medicine (Baltimore).* 2019;98:e14973.
- Zhang G, Cheng Y, Zhang Q, et al. ATX-LPA axis facilitates estrogen-induced endometrial cancer cell proliferation via MAPK/ERK signaling pathway. *Mol Med Rep.* 2018;17:4245-4252.
- Yun CC. Lysophosphatidic acid and Autotaxin-associated effects on the initiation and progression of colorectal cancer. *Cancers (Basel).* 2019;11:958.
- Si J, Su Y, Wang Y, Yan YL, Tang YL. Expressions of lysophosphatidic acid receptors in the development of human ovarian carcinoma. *Int J Clin Exp Med.* 2015;8:17880-17890.
- Quan M, Cui JJ, Feng X, Huang Q. The critical role and potential target of the autotaxin/lysophosphatidate axis in pancreatic cancer. *Tumour Biol.* 2017;39. doi:10.1177/1010428317694544
- Valdés-Rives SA, González-Arenas A. Autotaxin-lysophosphatidic acid: from inflammation to cancer development. *Mediators Inflamm.* 2017;2017:9173090.
- Tang X, Wuest M, Benesch MGK, et al. Inhibition of autotaxin with GLPG1690 increases the efficacy of radiotherapy and chemotherapy in a mouse model of breast cancer. *Mol Cancer Ther.* 2020;19:63-74.
- Iwaki Y, Ohhata A, Nakatani S, et al. ONO-8430506: a novel autotaxin inhibitor that enhances the antitumor effect of paclitaxel in a breast cancer model. *ACS Med Chem Lett.* 2020;11:1335-1341.
- Feng Y, Mischler WJ, Gurung AC, et al. Therapeutic targeting of the secreted lysophospholipase D autotaxin suppresses tuberculous sclerosis complex-associated tumorigenesis. *Cancer Res.* 2020;80:2751-2763.
- Desroy N, Housseman C, Bock X, et al. Discovery of 2-[[2-Ethyl-6-[4-[2-(3-hydroxyazetidin-1-yl)-2-oxoethyl]piperazin-1-yl]-8-methylimidazo[1,2-a]pyridin-3-yl]methylamino]-4-(4-fluorophenyl)thiazole-5-carbonitrile (GLPG1690), a first-in-class autotaxin inhibitor undergoing clinical evaluation for the treatment of idiopathic pulmonary fibrosis. *J Med Chem.* 2017;60:3580-3590.
- Geraldo LHM, Spohr T, Amaral RFD, et al. Role of lysophosphatidic acid and its receptors in health and disease: novel therapeutic strategies. *Signal Transduct Target Ther.* 2021;6:45.

31. Yang Y, Mou L, Liu N, Tsao MS. Autotaxin expression in non-small-cell lung cancer. *Am J Respir Cell Mol Biol*. 1999;21:216-222.
32. Shin E, Koo JS. Expression of proteins related to autotaxin-lysophosphatidate signaling in thyroid tumors. *J Transl Med*. 2019;17:288.
33. Chen J, Li H, Xu W, Guo X. Evaluation of serum ATX and LPA as potential diagnostic biomarkers in patients with pancreatic cancer. *BMC Gastroenterol*. 2021;21:58.
34. Jino N, Yoshida M, Hayashi K, et al. Autotaxin in ascites promotes peritoneal dissemination in pancreatic cancer. *Cancer Sci*. 2021;112:668-678.
35. Singh AD, Sisley K, Xu Y, et al. Reduced expression of autotaxin predicts survival in uveal melanoma. *Br J Ophthalmol*. 2007;91:1385-1392.
36. Balijepalli P, Sitton CC, Meier KE. Lysophosphatidic acid signaling in cancer cells: what makes LPA so special? *Cell*. 2021;10:2509.
37. Houben AJS, Moolenaar WH. Autotaxin and LPA receptor signaling in cancer. *Cancer Metastasis Rev*. 2011;30:557-565.
38. Albers HM, Dong A, van Meeteren LA, et al. Boronic acid-based inhibitor of autotaxin reveals rapid turnover of LPA in the circulation. *Proc Natl Acad Sci U S A*. 2010;107:7257-7262.
39. Benesch MG, Tang X, Maeda T, et al. Inhibition of autotaxin delays breast tumor growth and lung metastasis in mice. *FASEB J*. 2014;28:2655-2666.
40. Jia Y, Li Y, Xu XD, Tian Y, Shang H. Design and development of autotaxin inhibitors. *Pharmaceuticals (Basel)*. 2021;14:1203.
41. Maher TM, van der Aar EM, van de Steen O, et al. Safety, tolerability, pharmacokinetics, and pharmacodynamics of GLPG1690, a novel autotaxin inhibitor, to treat idiopathic pulmonary fibrosis (FLORA): a phase 2a randomised placebo-controlled trial. *Lancet Respir Med*. 2018;6:627-635.
42. Tang LH, Untch BR, Reidy DL, et al. Well-differentiated neuroendocrine tumors with a morphologically apparent high-grade component: a pathway distinct from poorly differentiated neuroendocrine carcinomas. *Clin Cancer Res*. 2016;22:1011-1017.
43. Yachida S, Vakiani E, White CM, et al. Small cell and large cell neuroendocrine carcinomas of the pancreas are genetically similar and distinct from well-differentiated pancreatic neuroendocrine tumors. *Am J Surg Pathol*. 2012;36:173-184.
44. Yamauchi Y, Kodama Y, Shiokawa M, et al. Rb and p53 execute distinct roles in the development of pancreatic neuroendocrine tumors. *Cancer Res*. 2020;80:3620-3630.

#### SUPPORTING INFORMATION

Additional supporting information can be found online in the Supporting Information section at the end of this article.

**How to cite this article:** Toyohara T, Yoshida M, Miyabe K, et al. Dual role of autotaxin as novel biomarker and therapeutic target in pancreatic neuroendocrine neoplasms. *Cancer Sci*. 2023;114:4571-4582. doi:[10.1111/cas.15980](https://doi.org/10.1111/cas.15980)